Cell Reports, Volume *32*

Supplemental Information

Structure in Neural Activity during Observed and Executed Movements Is Shared at the Neural Population Level, Not in Single Neurons

Xiyuan Jiang, Hemant Saggar, Stephen I. Ryu, Krishna V. Shenoy, and Jonathan C. Kao

Supplemental information

Analysis	Quantity	Putative single units	Putative single units, $R^2 > 0.3$	Threshold crossings
Observation vs execution tuning statistics	Number of recordings	41 to 83	19 to 52	95 to 192
	% of incgrt recordings in M1	47.4, 53.2 (35.0, 42.3)	70.5, 62.9 (62.7, 54.8)	43.7, 39.5 (34.8, 32.8)
	% of incgrt recordings in PMd	52.7, 43.7 (43.6, 41.6)	66.7, 54.3 (60.6, 52.6)	58.8, 40.4 (53.6, 27.1)
	Mean PD change (incgrt.)	108.8, 95.2 (110.1, 96.8)	97.4, 85.4 (101.8, 87.8)	108.6, 81.7 (108.7, 83.7)
Cross Proj	Obs var on 10 Ex PCs	40.0, 49.5	52.6, 63.7	47.8, 51.6
	Ex var on 10 Obs PCs	44.0, 48.2	51.2, 61.5	55.4, 55.6
	p-val Obs var > rand	0, 0	0, 0	0, 0
	p-val Ex var > rand	0, 0	0, 0	0, 0
subspace Opt (D=4)	Opt 1: var. Obs on Orth-Obs	92.4, 91.5	93.2, 89.5	81.6, 84.0
	Opt 1: var. Ex on Orth-Obs	96.0, 93.1	95.1, 91.3	90.0, 87.9
	Opt 1: var. Obs on Orth-Ex	15.9, 18.0	15.7, 22.0	22.5, 21.4
	Opt 1: var. Ex on Orth-Obs	10.3, 13.9	14.2, 17.7	13.1, 15.8
	Opt 1: acc. Obs on Orth-Ex	15.3, 21.3	19.3, 22.8	24.9, 28.1
	Opt 1: acc. Ex on Orth-Obs	72.7, 55.7	71.3, 57.2	89.5, 71.3
	Opt 2: var. Obs on Excl-Obs	64.1, 51.3	80.2, 66.8	59.2, 53.4
	Opt 2: var. Ex on Excl-Ex	47.2, 35.1	74.2, 59.0	43.8, 40.8
	Opt 2: acc. Obs on Excl-Obs	43.6, 44.4	45.9, 44.2	72.6, 58.3
	Opt 2: acc. Ex on Excl-Ex	87.9, 70.7	87.6, 70.6	97.7, 85.8
	Opt 3: var. Obs on Shared	52.8, 59.2	35.2, 47.3	54.2, 56.6
	Opt 3: var. Ex on Shared	66.3, 73.1	42.3, 50.2	69.1, 69.2
	Opt 3: acc. Obs on Shared	43.5, 40.7	24.6, 35.5	47.6, 42.9
	Opt 3: acc. Ex on Shared	88.1, 81.8	79.3, 73.5	96.0, 86.1
Congruent vs incongruent subspace composition	Excl-Obs var (cgrt, incgrt)	58.8, 60.2 (56.8, 58.3)	–	53.9, 71.8 (53.8, 70.6)
	Excl-Ex var (cgrt, incgrt)	41.2, 60.3 (40.9, 61.0)	–	44.1, 63.4 (42.2, 63.8)
	Shared Obs var (cgrt, incgrt)	63.3, 56.2 (63.5, 56.8)	–	63.1, 44.7 (64.1, 45.0)
	Shared Exe var (cgrt, incgrt)	69.6, 58.3 (70.9, 56.4)	–	68.0, 53.8 (69.2, 53.3)
jPCA	Ex R^2_{skew}	0.61	0.59	0.63
	Ex R^2_{best}	0.69	0.65	0.72
	Obs R^2_{skew}	0.36	0.36	0.44
	Obs R^2_{best}	0.45	0.45	0.56

Table S1. Mean statistics from the analyses in the main manuscript performed on putative single units, putative single with $R^2 > 0.3$, and threshold crossings (unsorted). Related to Fig 3, Fig 4. When two numbers are listed in a single entry for the first three analyses, the first number is for Monkey J, the second for Monkey L. For congruent vs incongruent subspace composition, these numbers reflect the averages across all datasets in both monkeys. Numbers on the left correspond to congruent neurons and numbers on the right correspond to incongruent neurons. Numbers in the parentheses are obtained after multiple comparision correction with the Benjamini–Hochberg procedure. For jPCA, these numbers reflect the average across all datasets in both monkeys. In the column 'Putative single units, $R^2 > 0.3$', subspace optimization results are obtained with $v = 0.05$ instead of $v = 0.01$ because the latter does not have enough neurons when computing the exclusive subspaces.

# of dimensions	Obs on Orth-Ex	Ex on Orth-Ex	Ex on Orth-Obs	Obs on Orth-Obs
5D	15.4, 17.9	95.6, 92.7	10.4, 13.7	92.2, 91.2
10D	15.4, 18.6	93.8, 91.2	10.5, 13.8	91.2, 90.3
15D	16.2, 19.2	92.8, 90.3	10.5, 14.1	90.7, 89.0
20D	16.3, 19.4	92.3, 89.3	10.7, 14.3	90.1, 87.7

Table S2. Normalized variance captured (%) with different subspace dimensions for subspace optimization addressing hypothesis 1, for Monkey J, L. Related to Fig 3E.

	$D = 4$			$D = 3$			$D = 2$		
Constraint	0.01	0.02	0.05	0.01	0.02	0.05	0.01	0.02	0.05
Excl-Obs, J	64.1	74.5	86.2	64.7	75.1	87.0	69.1	79.4	90.9
Excl-Obs L	51.3	64.5	79.3	52.6	65.8	80.6	52.4	66.1	81.2
Excl-Ex J	47.2	60.5	77.9	48.2	60.8	77.6	47.8	60.4	77.1
Excl-Ex, L	35.0	51.3	71.2	38.5	53.6	72.9	41.3	56.1	74.7
Acc., obs on Excl-Obs J	43.6	47.4	48.3	41.4	43.8	45.8	36.1	38.2	39.9
Acc., obs on Excl-Obs L	44.4	47.5	50.5	44.5	46.7	49.1	41.4	45.1	48.0
Acc., ex on Excl-Ex J	87.9	90.5	91.8	86.1	86.8	89.3	73.9	76.0	79.1
Acc., ex on Excl-Ex L	70.7	79.7	83.2	72.8	77.3	81.6	68.2	69.5	73.2

Table S3. Exclusive subspace normalized variance for different dimensions and opposite-context variance captured constraints. Related to Fig 4B.

	$D=4$			$D=3$			$D=2$		
Constraint	0.01	0.02	0.05	0.01	0.02	0.05	0.01	0.02	0.05
Obs in Shared, J	52.8	44.4	32.5	53.7	45.8	34.9	57.4	53.1	49.0
Obs in Shared, L	59.2	49.7	34.9	61.7	52.3	38.4	61.8	54.4	45.6
Ex in Shared, J	66.3	58.1	39.3	69.0	62.4	45.2	69.9	65.2	52.7
Ex in Shared, L	73.1	60.9	39.7	72.5	63.2	47.0	72.4	66.0	53.8
Acc., obs on Shared J	43.5	39.2	29.3	35.2	30.9	26.3	26.9	21.2	21.2
Acc., obs on Shared L	40.7	37.8	32.6	40.3	36.3	32.1	34.8	29.2	29.2
Acc., ex on Shared J	88.1	84.0	84.0	78.9	79.6	73.5	74.5	72.5	68.2
Acc., ex on Shared L	81.8	79.9	72.7	78.2	76.8	69.8	75.3	72.5	59.9

Table S4. Shared subspace normalized variance for different dimensions and opposite-context variance captured constraints. Related to Fig 4D.

Monkey	J	L	J	L	J	L
Population	all	all	M1	M1	PMd	PMd
Obs var on 10 Ex PCs	40	49.5	50.9	69.7	62.5	67
Ex var on 10 Obs PCs	44	48.2	55.1	61.5	59.3	71.5
p-val Obs var $>$ rand	0	0	0	0	0	0.0002
p-val Ex var $>$ rand	0	0	0	0.0987	0.0018	0
Opt 1: var. Obs on Orth-Obs	92.4	92.7	90.7	92.3	88.7	89.4
Opt 1: var. Ex on Orth-Obs	96	92.8	96	90.2	92.8	93.0
Opt 1: var. Obs on Orth-Ex	16	14.4	20.5	15.0	25.3	25.0
Opt 1: var. Ex on Orth-Obs	10.3	13.3	11.4	19.3	17.4	17.7
Opt 1: acc. Obs on Orth-Ex	15.3	23.9	16.3	23.1	11.9	21.8
Opt 1: acc. Ex on Orth-Obs	72.7	56.7	69.5	55.4	64.1	39.8
Opt 2: var. Obs on Excl-Obs	86.2	81.2	81.2	66.0	68.1	72.0
Opt 2: var. Ex on Excl-Ex	77.9	78.2	65.1	72.3	53.5	49.8
Opt 2: acc. Obs on Excl-Obs	48.3	58.9	39.3	47.0	28.5	32.6
Opt 2: acc. Ex on Excl-Ex	91.8	86.4	90.6	81.7	74.5	60.0
Opt 3: var. Obs on Shared	32.5	29.2	37.8	47.7	51.2	49.0
Opt 3: var. Ex on Shared	39.3	32.2	55.4	42.3	58.5	64.8
Opt 3: acc. Obs on Shared	29.3	36.5	23.7	33.8	20.0	32.9
Opt 3: acc. Ex on Shared	84.0	71.2	76.9	71.5	75.4	64.7

Table S5. Cross projection and subspace results for M1 and PMd, separately. Related to Fig 3 and Fig 4. Results are obtained by setting $v = 0.05$ instead of $v = 0.01$ when computing the exclusive subspaces, because the latter does not have enough neurons. Dataset **L140829** was excluded for the same reason.

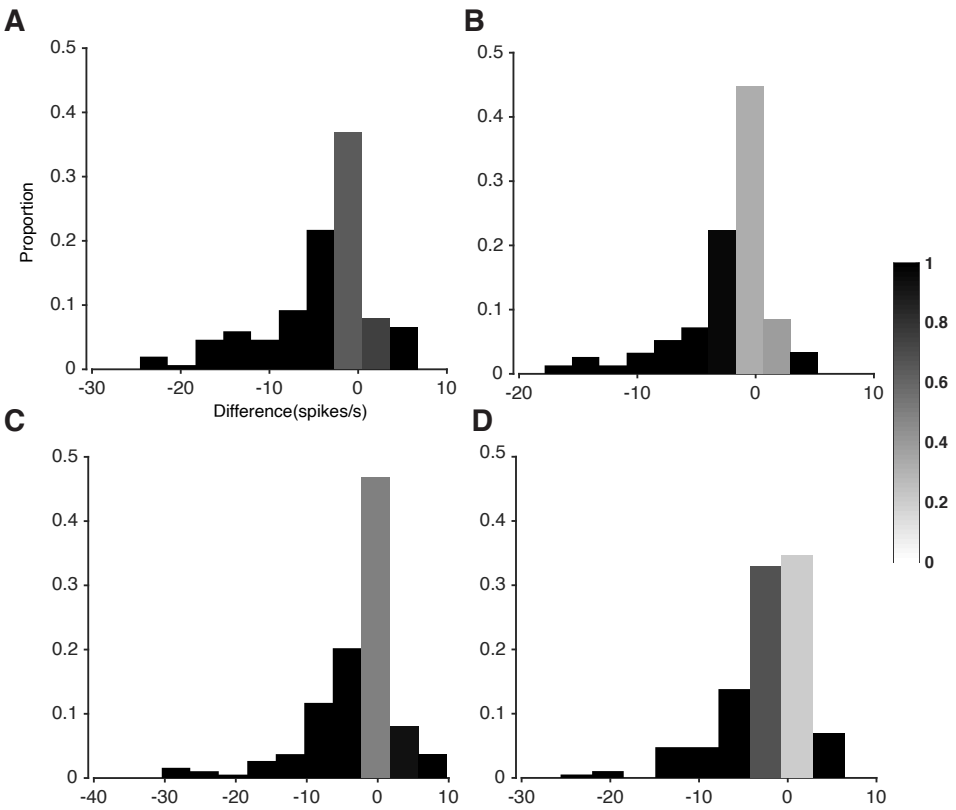

Figure S1. Tuning curve characteristics. Related to Fig 2. **(A)** Distribution of changes in baseline firing rate for Monkey J. **(B)** Distribution of changes in modulation depth for Monkey J. **(C, D)** Same as **(A, B)** but for Monkey L. Grayscale indicates the proportion of neurons with significant changes in each bin.

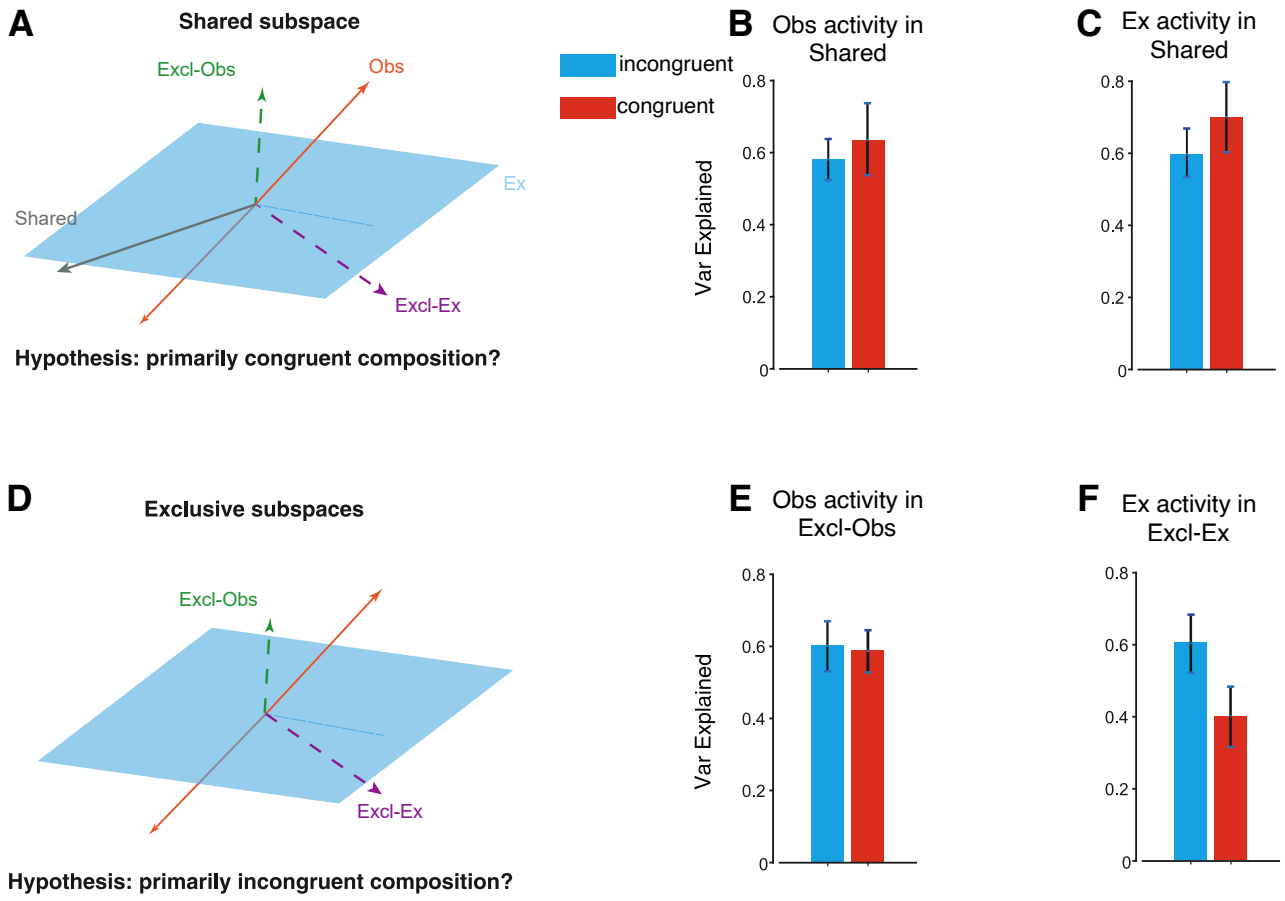

Figure S2. Exclusive and Shared subspace optimization with congruent and incongruent neurons. Related to Fig 4. **(A)** Illustration of the Shared subspace (gray) relative to the execution (blue) and observation (orange) subspaces. For all panels in this figure, dataset **L140829** was excluded because there were not sufficient number of units to do this analysis. **(B)** Captured observation variance (mean $\pm$ standard dev.) across all datasets for the Shared subspace. **(C)** Same as **(B)** but for execution variance. **(D)** Illustration of the Exclusive subspaces (one for execution in purple, one for observation in green) relative to prior described subspaces. **(E)** Captured observation variance (z-scored) across all datasets for the Excl-Obs subspace for only congruent (red) or incongruent (blue) neurons. **(F)** Same as **(E)** but for exclusive variance in the Excl-Ex subspace.

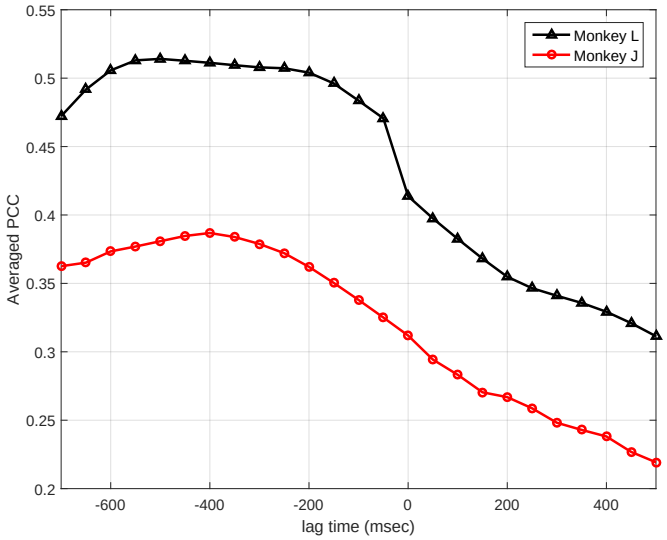

Figure S3. Decoding cursor position at various lags. Related to Fig 2. Average Pearson Correlation Coefficient (PCC) between the cursor position and decoded cursor position for optimal linear estimator decoders constructed at various lags between neural activity and kinematics. Negative lags indicate neural activity precedes kinematics. Neural activity was smoothed using a causal Gaussian kernel with a standard deviation of 100 ms (each time bin width = 50 ms). PCC between the predicted and actual cursor coordinate was calculated for each lag and then averaged across trials and (x, y) coordinates.

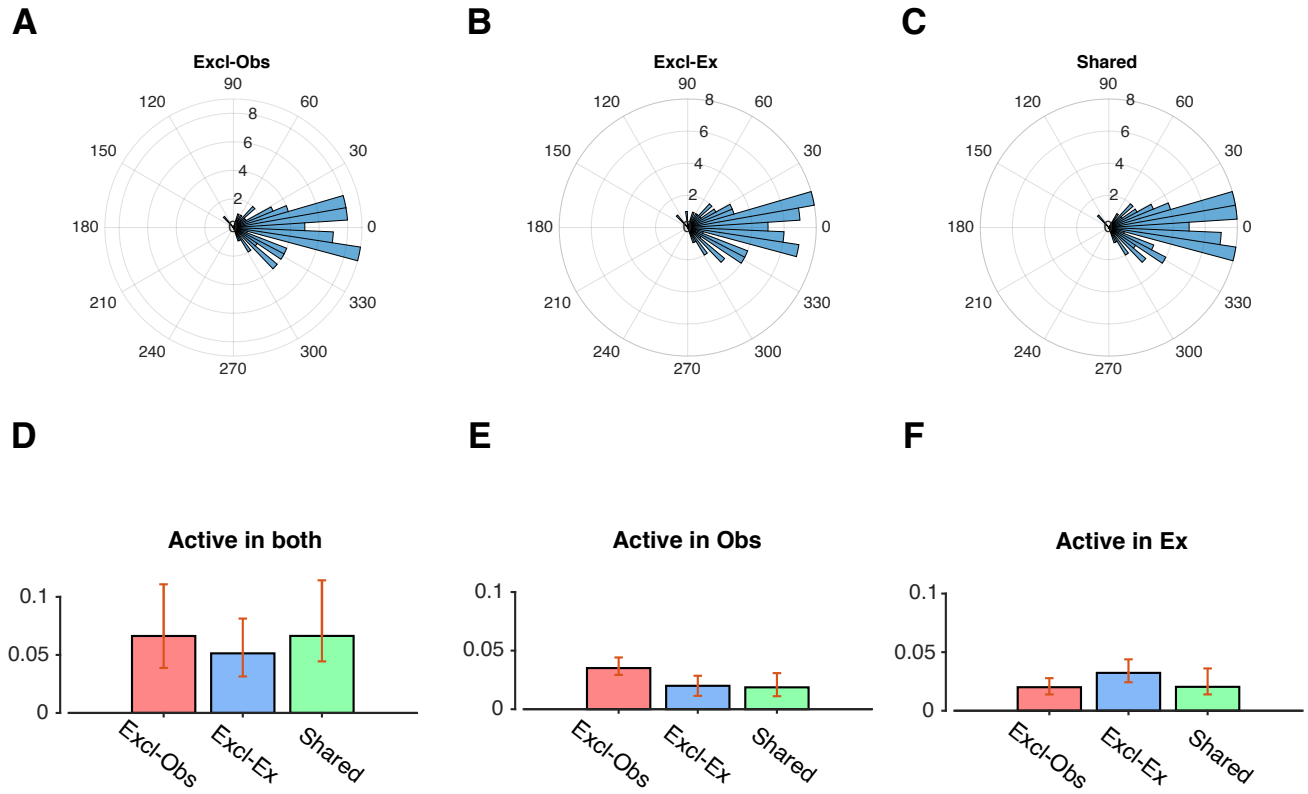

Figure S4. Neuron PD changes and subspace contributions. Related to Fig 5. **(A, B, C)** PD changes of congruent neurons with a subspace contribution of at least 0.01 in the **(A)** Excl-Obs, **(B)** Excl-Ex, and **(C)** Shared subspaces for neurons with a tuning $R^2 > 0.3$. Related to Fig 5. The average absolute PD shifts across these congruent neurons for the Shared, Excl-Obs, and Excl-Ex subspaces were 21.4, 22.0, and 23.9 degrees, respectively. These differences were not significant ($p = 0.84$ for Excl-Obs vs Shared, $p = 0.5$ for Excl-Ex vs Shared, $p = 0.62$ for Excl-Ex vs Excl-Obs, Watson-Williams multi-sample test for equal means (Berens & Velasco, 2009)). When considering the entire population (including those with $R^2 < 0.3$, the average PD shifts for the Shared, Excl-Obs, and Excl-Ex subspaces were 41.0, 43.1, and 45.6 degrees, respectively. These differences were also not significant ($p = 0.66$ for Excl-Obs vs Shared, $p = 0.33$ for Excl-Ex vs Shared, $p = 0.60$ for Excl-Ex vs Excl-Obs). **(D, E, F)** Median subspace contributions of neurons (with 25th and 75th percentiles) to the Exclusive and Shared subspaces. Neurons can be active in both contexts if their mean firing rate is $\bar{FR} > 2$ spikes/s in both contexts (65.8% of neurons), active only in observation ($\bar{FR} > 2$ spikes/s in observation and $\bar{FR} <= 2$ spikes/s in execution, 3.5% of neurons), or active in execution ($\bar{FR} > 2$ spikes/s in execution and $\bar{FR} <= 2$ spikes/s in observation, 15.8% of neurons). **(D)** Neurons active in both execution and observation contribute to all subspaces (medians with error bars denoting the 25th and 75th percentiles). **(E)** Neurons active only in observation contribute more to the Excl-Obs space, but not as much to the Excl-Ex and Shared subspaces. **(F)** Neurons active only in execution contribute more to the Excl-Ex space, but not as much to the Excl-Obs and Shared subspaces.

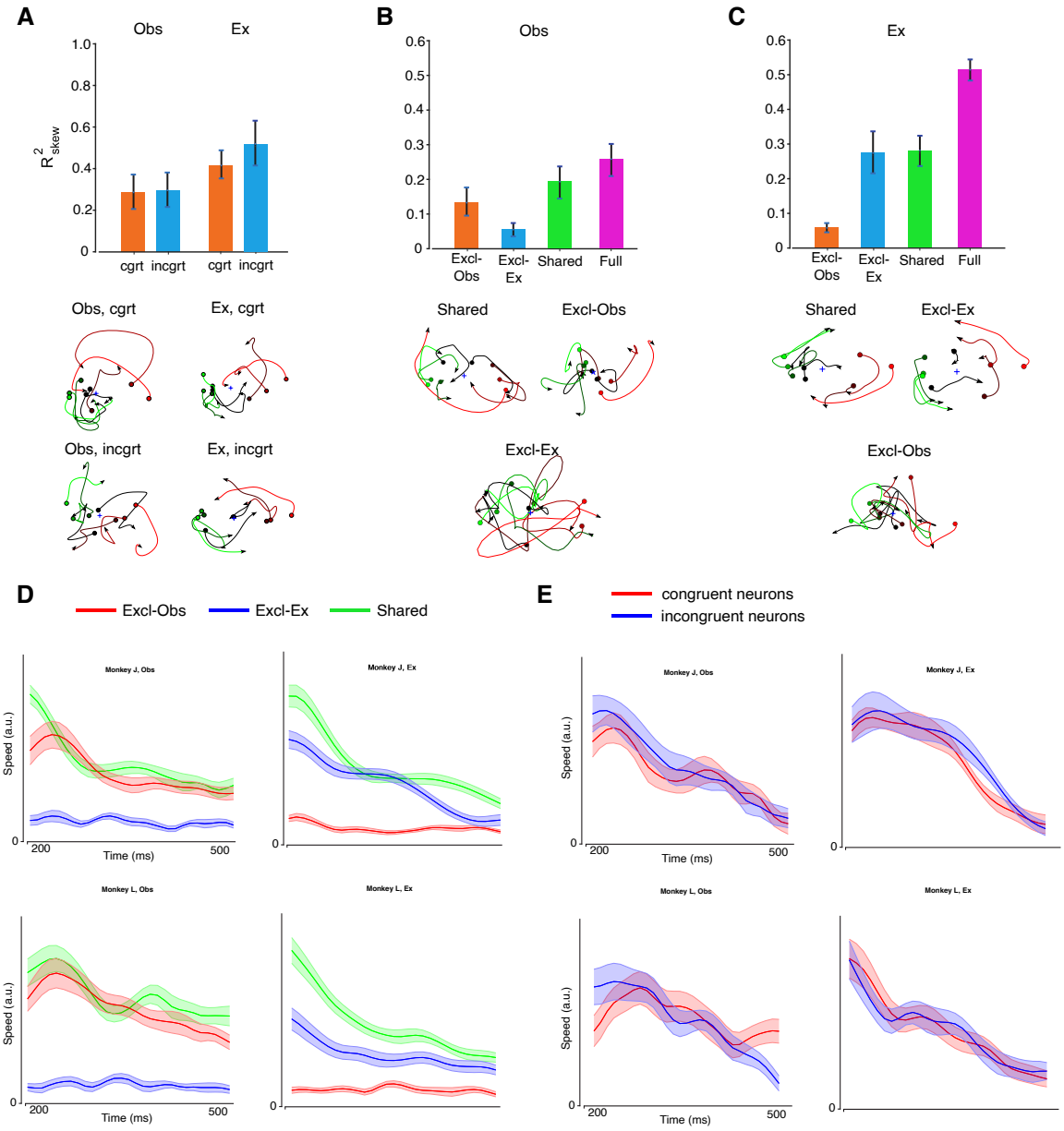

Figure S5. Neural dynamics in subpopulations and subspaces. Related to Fig 6. We quantified the rotational dynamics in **(A)** congruent versus incongruent subpopulations, and **(B, C)** in Shared and Exclusive subspaces. Examples trajectories are also shown. **(A)** We did not find a significant difference in rotational dynamics between congruent and incongruent subpopulations in either observation or execution contexts. In observation: the mean R^2_{skew} was 0.29 (0.27) for incongruent (incongruent) neurons with $p = 0.78$, bootstrap. In execution: the mean R^2_{skew} was 0.51 (0.42), with $p = 0.50$. **(B)** Rotational dynamics in Excl-Ex had significantly less rotational dynamics than Shared ($p < 0.05$, Wilcoxon rank sum test). Shared and Excl-Obs did not have significantly different rotational dynamics ($p = 0.31$). Excl-Ex and Excl-Obs did not have significantly different rotational dynamics ($p = 0.09$). Note that these R^2_{skew} values are smaller than the ones reported in the paper because we performed them in 4D (not 6D) since our subspace optimizations were for 4D subspaces. **(C)** Same as **(B)** but for execution activity. Excl-Obs had significantly less rotational dynamics than Shared ($p < 0.05$). Shared and Excl-Ex did not have significantly different rotational dynamics ($p = 1$). Excl-Obs and Excl-Ex did not have significantly different rotational dynamics ($p = 0.14$). **(D, E)** Neural trajectory speeds in different subspaces and subpopulations, in **(D)** Excl-Obs, Excl-Ex and Shared subspaces, and **(E)** in the congruent and incongruent subpopulations. Neural trajectory speed decreaess in the Shared and within-context Exclusive subspace, but not in the opposite-context Exclusive subspace.

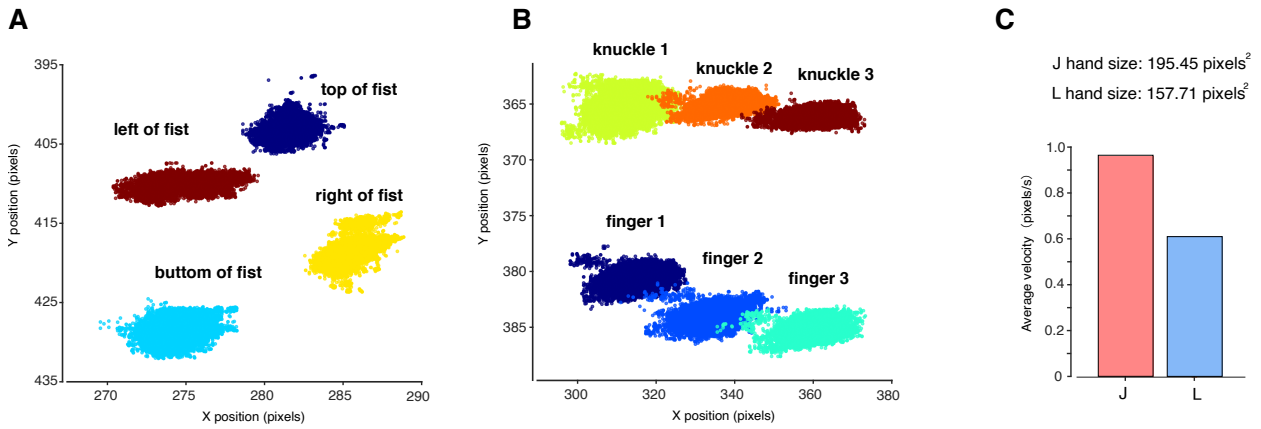

Figure S6. DeepLabCut tracking of the monkey's hand during a representative observation experiment. Related to Fig 2B. **(A)** We tracked Monkey J's hand, which formed a fist, during experiments. The approximate area of his hand on video was 195 pixels^2. Scatter of individual pixels is due to precision in DeepLabCut; when we watched these videos, we observed no significant overt movements. Importantly, in this panel, there were no deviations of the digits that were close to the size of the monkey's hand, even though the relatively larger size of our restraints meant such large hand movements were possible. **(B)** Tracking of Monkey L's hand. Monkey L's hand was open, and therefore we could track his knuckles and fingers. The area of his hand on video was approximately 158 pixels^2. **(C)** The average velocity of these points were 0.97 for Monkey J and 0.61 for Monkey L. This small velocity is attributable to DeepLabCut precision.